PROCEEDINGS OF SCIENCE

Equations of state of dense matter for neutron-star modelling and inference

Anthea F. Fantina[a,*] **and Francesca Gulminelli**[b]

[a] *Grand Accélérateur National d'Ions Lourds (GANIL), CEA/DRF – CNRS/IN2P3, Boulevard Henri Becquerel, 14076 Caen, France*

[b] *Université de Caen Normandie, ENSICAEN, CNRS/IN2P3, LPC Caen UMR6534, 14000 Caen, France*

E-mail: anthea.fantina@ganil.fr, gulminelli@lpccaen.in2p3.fr

The equation of state (EoS) is a needed input for neutron-star (NS) modelling allowing one to connect microphysics inputs with global NS properties. In this contribution, we briefly present the EoS modelling for NSs, particularly focusing on a meta-model-based approach, and discuss the importance of a consistent and unified approach. We show that employing a fixed but inconsistent model for the lower density region causes (small) errors and underestimates the uncertainties in the estimation of global NS properties. This confirms our previous findings and underlines the relevance of a consistent approach in NS modelling and inference.

10th International Conference on Quarks and Nuclear Physics (QNP2024)
8-12 July, 2024
Barcelona, Spain

*Speaker

PoS(QNP2024)153

1. Introduction

Born in the aftermath of supernova explosions, neutron stars (NSs) are among the most compact objects in the Universe, with a mass of $\approx 1 - 2M_\odot$ ($M_\odot$ being the solar mass), a radius of about 10 km, and central densities that can reach several times nuclear saturation density, $n_{\rm sat} \approx 0.16\,{\rm fm}^{-3}$ [1]. The first multi-messenger detection of a binary NS merger, the event GW170817 [2], in addition to the precise NS mass measurements around $2M_\odot$ [3–5] and the recent quantitative estimation of the mass–radius relation obtained from NICER measurements (see Refs. [6, 7] and refs. therein) have, in the last few years, pushed the study of dense-matter properties in NSs. The more and more numerous observations expected from the LIGO-Virgo-KAGRA collaboration, as well as those foreseen from the planned third-generation detectors and instruments, are expected to provide valuable data from which new information on the structure and composition of NSs can be inferred.

To reliably connect astrophysical observations to the properties of dense matter in the NS interior, an equation of state (EoS), that is, the functional relation between the pressure and the mass-energy density, is needed. Indeed, under the assumption of general relativity, the relation between static properties of cold beta-equilibrated NSs, which is a valid assumption for mature isolated NSs or coalescing NSs in their inspiral phase, and the underlying microphysics mainly relies on the knowledge of the EoS. The determination of the NS EoS is a challenge, because of the different phases of matter (from neutron-rich clustered matter in the crust to homogeneous matter in the core) and the range of thermodynamic conditions encountered in these astrophysical objects. From the nuclear-physics side, current constraints on the EoS come from terrestrial experiments, mainly probing density around saturation and rather symmetric matter, and ab-initio calculations ([8–10] for a review). The latter ones, like those based on the chiral effective field theory (χ-EFT), have undergone enormous progress, and are now able to quantify uncertainties on the infinite-matter EoS. These models can constitute powerful constraints, particularly concerning predictions for pure neutron matter, but cannot be employed in all NS regions. Phenomenological models, most of which rooted on the nuclear energy-density functional theory, have thus to be applied instead. Constraints on the EoS also come from astrophysical data; in this respect, most NS studies and inference of NS properties from observations, specifically from gravitational-wave data, are done with so-called non-unified EoSs, i.e. different models for the different NS regions (outer and inner crust, and core) are employed. In particular, because of the complexity related to the calculation of the inhomogeneous region and based on the idea that the crust EoS is relatively well constrained and has a little effect on NS macroscopic properties, often a unique EoS crust model is used. However, a thermodynamically consistent description of all NS regions is important for (dynamical) simulations since the (ad-hoc) matching of different EoSs may lead to spurious instabilities and uncertainties in the predictions of NS properties [11–14]. We recently proposed a numerical tool, the Crust Unified Tool for Equation-of-state Reconstruction (`CUTER`), that provides a unified and consistent NS EoS starting from a high-density beta-equilibrated EoS for the NS core [14].

In this work, we briefly present the EoS modelling for NSs in Sect. 2, with a particular focus on a meta-model-based approach. To evaluate the importance of the use of a consistent and unified EoS in NS modelling and inference, we extend the study of Ref. [14] and perform additional Bayesian analyses. We compare the NS properties thus obtained with those calculated employing a unique EoS model for the low-density part in Sect. 3. Finally, we draw our conclusion in Sect. 4.

2. Neutron-star equation of state

For cold, mature, and non-accreting NSs, the temperature (typically below 1 MeV) is lower than typical nuclear energies thus the zero-temperature approximation can be adopted in computing the EoS. This assumption, together with the beta-equilibrium condition, makes the EoS dependent on the (energy) density only (see Refs. [8, 9, 15] for a review and discussion on so-called 'general-purpose' EoSs). Even in this case, the uncertainties in the EoS remain large, particularly as density increases. Indeed, for the outer crust (corresponding to the first few hundreds metres under the NS surface) the only nuclear inputs in the calculation of the EoS and composition are nuclear masses (either experimentally measured or theoretically calculated) thus the model dependence is relatively small and only affects the deeper layers, where masses of neutron-rich nuclei have to be determined from theoretical mass models. In the inner crust (from the so-called neutron drip up to the crust–core transition, at about $0.5n_{\rm sat}$), the presence of neutron-rich clusters in a background of electrons and unbound neutrons makes the EoS model dependent, both on the underlying functional and the many-body method used. In the core, the possible appearance of non-nucleonic degrees of freedom highly increases the uncertainties. As illustrative examples, a collection of beta-equilibrated zero-temperature NS EoSs is plotted in Fig. 1, using data taken from the `CompOSE` database [15]: the left panel shows different unified nucleonic EoSs in the crust-core density regime (changes of slope indicate the transition from the outer to the inner crust and from the crust to the core), while the right panel displays different EoSs (all of which — except PCP-BSk24, GPPVA-DD2, and GMSR-H1 — include heavy baryons or a phase transition to quark matter) in the core. As expected, the largest spread is indeed observed at high densities in the NS core. In view of these uncertainties and of the unknown composition in the core, several works employ purely agnostic models (either parametric, like piecewise polytropes or speed-of-sound models, or non-parametric, like Gaussian process) to construct (phenomenological) EoSs. These approaches do not rely on any description of the underlying microphysics and are only subject to general physics constraints such as causality and thermodynamic stability. However, these powerful tools, widely used to extract the nuclear EoS from gravitational waveforms (see e.g. Ref. [16] and refs. therein), cannot be used, for example, for applications requiring the knowledge of the NS composition, such as NS cooling simulations.

An alternative approach to extract information on the structure and properties of dense matter is constituted by EoS parametrisations covering the parameter space of effective nuclear models. This can be achieved by using the so-called nucleonic meta-modelling, i.e. by introducing a flexible energy functional able to reproduce existing effective nucleonic models and to interpolate between them. Following Ref. [17], we write the energy per particle of nucleonic matter depending on the baryon density n_B and asymmetry $\delta = (n_n - n_p)/n_B$, with $n_{n(p)}$ the neutron (proton) density, as

$$e_{\rm nuc}(n_B, \delta) = t^{\star}_{\rm FG}(n_B, \delta) + e_{\rm is}(n_B) + e_{\rm iv}(n_B)\delta^2 \,, \tag{1}$$

where the kinetic term $t^{\star}_{\rm FG}$ includes the dominant deviation to the parabolic approximation as well as the effective mass contribution and the residual isoscalar $e_{\rm is}$ and isovector $e_{\rm iv}$ terms contain the most important model dependence. The latter ones can be written as a Taylor expansion in $x = (n_B - n_{\rm sat})/(3n_{\rm sat})$ up to order N around the saturation density $n_{\rm sat}$ as:

$$e_{\rm is(iv)}(n_B) = \sum_{k=0}^{N} \frac{v_k^{\rm is(iv)}}{k!} x^k u_k(x) \,, \tag{2}$$

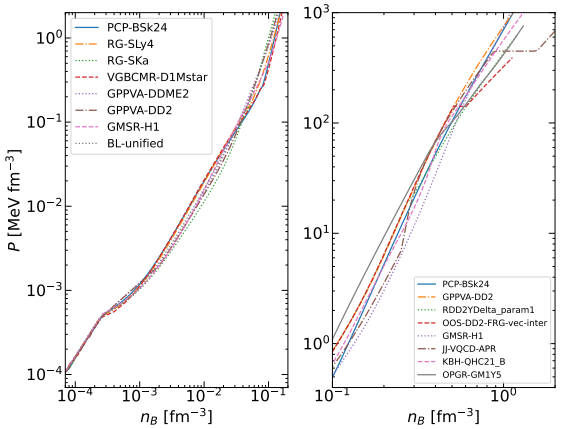

Figure 1: Pressure versus baryon number density for different EoS models taken from the `CompOSE` database [15] (see text for details).

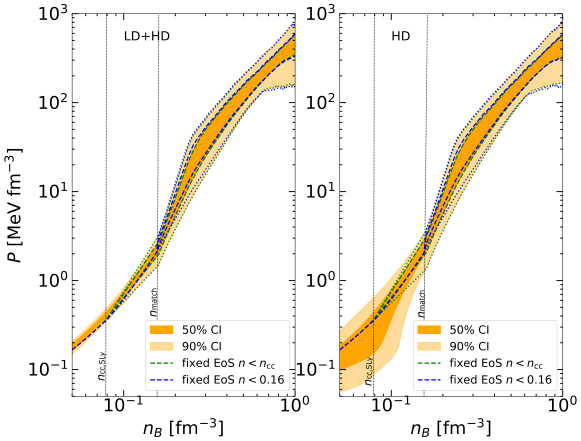

Figure 2: Posterior distribution for the EoS when LD+HD constraints or only HD constraints are applied (see text for details).

where the function $u_k = 1-(-3x)^{N+1-k}\exp(-bn_B/n_{\rm sat})$ (with $b = 10\ln 2$) ensures the correct zero-density limit, and the parameters $v_k^{\rm is(iv)}$ are directly connected to the so-called isoscalar (isovector) nuclear empirical parameters (NEP) ($\{E_{\rm sat(sym)}, (L_{\rm sym},)K_{\rm sat(sym)}, Q_{\rm sat(sym)}, Z_{\rm sat(sym)}\}$ for $N = 4$), given by the successive derivatives of the energy functional at saturation (see Refs. [14, 17–19] for details). In this way, it is possible to reproduce given functionals by assigning the corresponding values of the NEP, or sample them to generate (semi-agnostic) EoS sets in a statistical analysis. For a correct computation of the NS EoS, a treatment of the clustered (inhomogeneous) crust is required. To this aim, we used a compressible liquid-drop model for the ions, where the bulk energy was complemented with Coulomb, surface, and curvature contributions (see Refs. [14, 18, 19] for details). The complete parameter set of the model thus consists of 13 bulk parameters plus 5 surface parameters, which are consistently determined from a χ^2 fit to the experimental masses from the Atomic Mass Evaluation (AME) [20]. The EoS and composition are then variationally computed for each full set of parameters by minimising the energy density of the system under the condition of baryon number conservation, charge neutrality and beta equilibrium holding. In this work, only spherical clusters were considered (see e.g. Refs. [19] for a discussion on the so-called 'pasta' phases).

3. Numerical results for the EoS and NS properties

To assess the theoretical uncertainties in the EoS and the impact on the NS properties, we performed a Bayesian analysis, as described in Ref. [14]. The nuclear meta-modelling is run at order $N = 4$ up to a given baryon density $n_B = n_{\rm match}$, and the NEP $\{n_{\rm sat}, E_{\rm sat,sym}, L_{\rm sym}, K_{\rm sat,sym}, Q_{\rm sat,sym}, Z_{\rm sat,sym}\}$, together with the nucleon effective mass, the effective mass isosplit, and the b parameter are sampled from a uniform prior (see Table 4 in [14]). To account for the limited knowledge of the high-density part of the EoS and the possible occurrence of phase transitions not accounted for in a pure nucleonic (meta-)model, we matched a piecewise polytrope (with

a maximum of 5 polytropes) after $n_{\rm match}$. The transition densities among polytropes (and each polytropic index) are randomly drawn in the interval $[n_{\rm match}, 1.6\ {\rm fm}^{-3}]$ ($[0, 8]$). In this work, we set $n_{\rm match} = 0.16\ {\rm fm}^{-3}$, because we think that allowing for phase transitions below the saturation density would be rather unrealistic. Each piecewise polytrope is calculated until causality is reached.

Once the EoS is calculated, the static properties of a NS can be computed through the Tolmann-Oppenheimer-Volkoff equations [21], that allow the determination of the NS radius R and mass M. Moreover, the tidal deformability Λ is calculated as $\Lambda = (2/3)\ k_2\ (GM/(Rc^2))^{-5}$, k_2, G and c being the tidal Love number, the gravitational constant, and speed of light, respectively [22] (see Ref. [14] for complete expressions used in this work). The posterior distributions of the observables $\mathcal{Y}$ under the set of constraints $\mathbf{c}$ are obtained by marginalizing over the EoS parameters as

$$P(\mathcal{Y}|\mathbf{c}) = \prod_{k=1}^{N_{\rm par}} \int_{X_k^{\rm min}}^{X_k^{\rm max}} dX_k P(\mathbf{X}|\mathbf{c}) \delta(\mathcal{Y} - \mathcal{Y}(\mathbf{X}))\ , \tag{3}$$

where $N_{\rm par}$ is the number of parameters in the model (i.e. the NEP plus the polytrope parameters), and the posterior distribution of the parameters $\mathbf{X}$ conditioned by the likelihood of the different constraints $\mathbf{c}$ is given by $P(\mathbf{X}|\mathbf{c}) \propto P(\mathbf{X}) \prod_k P(c_k|\mathbf{X})$, where $P(\mathbf{X})$ is the prior. In this study, the following constraints are considered (see Ref. [14] for details): (i) the probability of each model (i.e. of each parameter set) is quantified by a Gaussian weight on the quality of the reproduction of the experimental nuclear masses [20]; (ii) at low density (LD), models are selected through a strict filter from the $\chi-$EFT calculations of the energy per nucleon of symmetric nuclear matter and pure neutron matter of Ref. [23] (the energy bands are enlarged by 5%). This constraint is applied in the interval from $0.02\ {\rm fm}^{-3}$ to $n_{\rm match}$; (iii) at high density (HD), causality, thermodynamic stability, non-negative symmetry energy at all densities where the meta-model is applied are imposed; in addition, the EoS has to support $\sim 2M_\odot$ NSs [4] (the associated likelihood is defined as a cumulative Gaussian distribution function). In Ref. [14], constraints from NICER [24, 25] and GW170817 [26] were also included, but were not considered here.

The resulting posterior EoS posterior is shown in Fig. 2: the yellow shaded areas represent the 50% (dark) and 90% (light) confidence intervals, while the curves correspond to the 50% (dashed lines) and 90% (dotted lines) confidence intervals for the EoS models calculated employing a unique EoS until the crust-core transition density $n_{\rm cc}$ (green lines) or until $n_{\rm match}$ (blue lines). We chose as unique EoS (crust plus eventually part of the core) that based on the SLy4 functional [27] because of its wide application to NS modelling and inference analyses (see e.g. Refs. [28, 29]). In the left panel, both LD filter from the $\chi-$EFT calculations and HD constraints, are applied. In the right panel, only HD filters have been applied, enlarging, as expected, the uncertainties in the lower density region, as already noticed in Ref. [30]. We can see that at high density the EoSs coincide, by construction[1]. When the additional polytrope is built between $n_{\rm cc}$ and $n_{\rm match}$ (indicated by vertical lines), the EoS remains smooth and partially retains the outer-core uncertainties. On the other hand, when the unique EoS is glued at $n_{\rm match}$, jumps in pressure are possible, although these remain relatively small because the SLy4 EoS agrees well with our posterior (yellow bands).

[1]The same posterior for the polytropic EoS resulting from the consistent EoS set was used when the unique low-density EoS is employed. The polytropic EoS is matched ensuring pressure monotonicity. When the unique EoS is calculated until the corresponding crust-core transition density $n_{\rm cc}$ ($n_{\rm cc,SLy} = 0.08\ {\rm fm}^{-3}$ for the SLy4 model, as indicated by the left vertical lines in Fig. 2), an additional polytrope is added between $n_{\rm cc}$ and $n_{\rm match}$; see Ref. [14] for details.

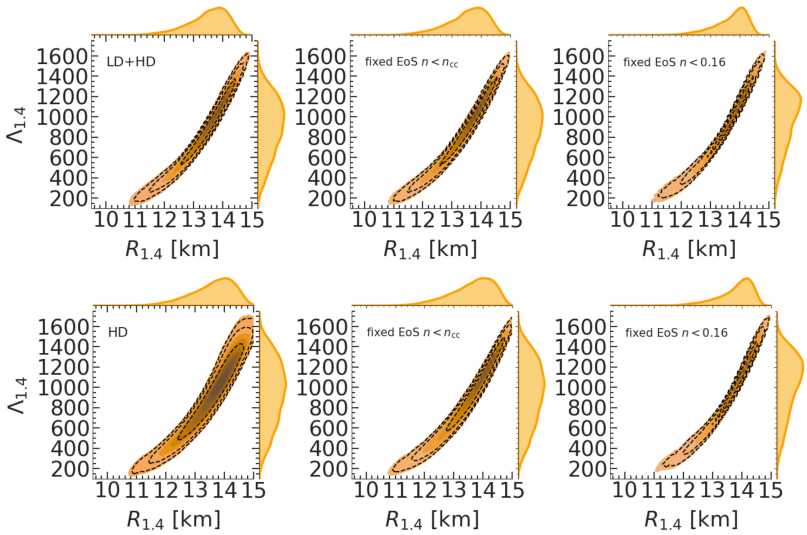

Figure 3: Joint probability density plots of dimensionless tidal deformability and radius for a $M = 1.4M_\odot$ NS, when LD+HD (top panels) or only HD (lower panels) filters are applied (see text for details).

As illustrative examples, the predictions for the radius and tidal deformability of a $1.4M_\odot$ NS corresponding to the EoSs shown in Fig. 2 are plotted in Fig. 3. As already noticed in Ref. [14], the median values of the global NS properties are not very much affected by the use of the unique crust (middle panel) when both LD and HD filters are considered. However, when the unique EoS is employed until $n_{\rm match}$ (right panel), although the median values do not change significantly (a few % and up to 10% for $\Lambda_{1.4}$), the uncertainties in the determination of the NS properties are underestimated. In Ref. [14] it was also pointed out that the small difference between the unique crust and the consistent treatment is largely influenced by the LD filter imposed on the EoS which strongly constrains the EoS for densities in the crust region. This is demonstrated in the lower panels of Fig. 3, where one can see that, although the average values are again not much affected by the use of a unique low-density EoS model (the difference being also in this case of a few %), the uncertainties are, and this is already noticeable when the unique EoS is applied until the crust-core transition density (middle panel). Indeed, the median and 68% confidence intervals for $R_{1.4}$ are $13.57^{+0.54}_{-0.81}$ km ($13.83^{+0.38}_{-0.75}$ km) when LD+HD filters are applied (when the unique EoS is used until $n_{\rm match}$), and $13.71^{+0.60}_{-0.89}$ km ($13.92^{+0.39}_{-0.76}$ km) when only HD filters are applied. For $\Lambda_{1.4}$, the median and 68% confidence intervals are 925^{+274}_{-332} (1025^{+226}_{-349}) when LD+HD filters are applied (when the unique EoS is used until $n_{\rm match}$), and 971^{+314}_{-362} (1073^{+243}_{-372}) when only HD filters are applied. The impact of the unique low-density EoS is particularly visible for larger values of radii and tidal deformabilities, that is, for lower NS masses, as one may expect since for these NSs the crust is expected to contribute in a more important way. This is shown in Fig. 4, that illustrates the joint probability for the radius and tidal deformability for $1M_\odot$ NS.

4. Conclusions

In this work, we have presented the EoS for NS modelling and inference, with particular focus on a meta-model-based approach. Using a Bayesian analysis and employing a piecewise polytrope

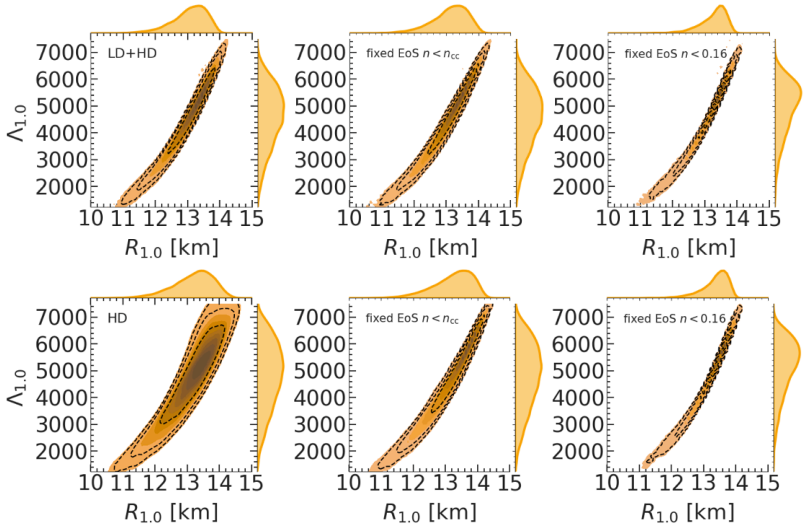

Figure 4: Same as in Fig. 3 for a $1.0 M_\odot$ NS.

at high density to account for the possible appearance of non-nucleonic degrees of freedom and phase transitions in the NS core, we discussed the impact of the use of a unified and consistent EoS model instead of a unique EoS at lower density. We show that the use of a fixed crust EoS model does not yield noticeable differences in the NS global properties, if the employed unique model is matched consistently at the corresponding crust-core transition and describes reasonably well the crust, confirming the findings in Ref. [14]. However, the use of non-unified EoSs and a fixed crust reduces the width of the distributions, particularly if the strict filter imposed on the EoS by the χ−EFT results is relaxed. This underlines, on the one side, the importance of a correct estimation of the systematic uncertainties in the theoretical calculations, and, on the other hand, the relevance of employing a consistent EoS in NS modelling and inference schemes to properly assess the associated uncertainties.

Acknowledgments

This work has been partially supported by the IN2P3 Master Project MAC and the CNRS IRP "Origine des éléments lourds dans l'univers: Astres Compacts et Nucléosynthèse (ACNu)". We also thank M. Oertel for helpful comments.

References

[1] P. Haensel, A. Y. Potekhin, D. G. Yakovlev, *Neutron Star I: Equation of State and Structure*, Springer, Berlin 2007

[2] B. P. Abbott et al., *Phys. Rev. Lett.* **119** (2017) 161101

[3] P. B. Demorest, T. Pennucci, S. M. Ransom, et al., *Nature* **467** (2010) 1081

[4] J. Antoniadis, P. C. C. Freire, N. Wex, et al. *Science* **340** (2013) 1233232

[5] H. T. Cromartie, E. Fonseca, S. M. Ransom, et al., *Nat. Astron.* **4** (2020) 72

[6] T. Salmi, S. Vinciguerra, D. Choudhury, et al., *ApJ* **941** (2022) 150

[7] S. Vinciguerra, T. Salmi, A. L. Watts, et al., *ApJ* **961** (2024) 62

[8] M. Oertel, M. Hempel, T. Klähn, S. Typel, *Rev. Mod. Phys.* **89** (2017) 015007

[9] G. F. Burgio, A. F. Fantina, *Astrophys. Space Sci. Lib.* **457** (2018) 255

[10] A. F. Fantina, F. Gulminelli, *J. Phys. Conf. Ser.* **2586** (2023) 012112

[11] M. Fortin, C. Providência, Ad. R. Raduta, et al., *Phys. Rev. C* **94** (2016) 035804

[12] L. Suleiman, M. Fortin, J. L. Zdunik, P. Haensel, *Phys. Rev. C* **104** (2021) 015801

[13] M. Ferreira, C. Providência, *Universe* **6** (2020) 220

[14] P. J. Davis, H. Dinh Thi, A. F. Fantina, et al., *A&A* **687** (2024) A44

[15] CompOSE Core Team, S. Typel et al., *Eur. Phys. J. A* **58** (2022) 221; https://compose.obspm.fr

[16] R. Essick, I. Legred, K. Chatziioannou, et al., *Phys. Rev. D* **108** (2023) 043013

[17] J. Margueron, R. Hoffmann Casali, F. Gulminelli, *Phys. Rev. C* **97** (2018) 025805

[18] T. Carreau, F. Gulminelli, J. Margueron, *Eur. Phys. J. A* **55** (2019) 188

[19] H. Dinh Thi, T. Carreau, A. F. Fantina, F. Gulminelli, *A&A* **654** (2021) A114

[20] M. Wang, W. J. Huang, F. G. Kondev, et al., *Chin. Phys. C* **45** (2021) 030003

[21] R. C. Tolman, *Phys. Rev.* **55** (1939) 364; J. R. Oppenheimer, G. M. Volkoff, *Phys. Rev.* **55** (1939) 374

[22] T. Hinderer, B. D. Lackey, R. N. Lang, J. S. Read, *Phys. Rev. D* **81** (2010) 123016

[23] C. Drischler, K. Hebeler, A. Schwenk, *Phys. Rev. C* **93** (2016) 054314

[24] T. E. Riley et al., *ApJ* **887** (2019) L21; *ApJ* **918** (2021) L27

[25] M. C. Miller et al., *ApJ* **887** (2019) L24; *ApJ* **918** (2021) L28

[26] B. P. Abbott et al. *Phys. Rev. X* **9** (2019) 011001

[27] E. Chabanat, P. Bonche, P. Haensel, et al., *Nucl. Phys. A* **627** (1997) 710; F. Douchin, P. Haensel, *A&A* **380** (2001) 151

[28] R. Essick, P. Landry, D. E. Holz, *Phys. Rev. D* **101** (2020) 063007

[29] R. Essick, I. Tews, P. Landry, et al., *Phys. Rev. C* **102** (2020) 055803

[30] H. Dinh Thi, C. Mondal, F. Gulminelli, *Universe* **7** (2021) 373